Age Estimation Based on Facial Images Using Hybrid Features and Particle Swarm Optimization

2021 11th International Conference on Computer Engineering and Knowledge (ICCKE) | 978-1-6654-0208-8/21/$31.00 ©2021 IEEE | DOI: 10.1109/ICCKE54056.2021.9721496

1st Niloufar Mehrabi
Department of Artificial Intelligence Engineering
Istanbul Aydin University
Istanbul, Turkey
niloufarmehrabi@stu.aydin.edu.tr

2nd Sayed Pedram Haeri Boroujeni
Department of Artificial Intelligence Engineering
Istanbul Aydin University
Istanbul, Turkey
sayedpedramboroujeni@stu.aydin.edu.tr

***Abstract*—Face images provide significant biological information. Face age estimation is one of the primary research directions in face images. The appearance of the face changes dynamically, and these changes are influenced by a variety of factors such as light, aging, makeup, beard, etc. The human face has many characteristics, including emotions, sex, race, age, etc. Face age estimation has numerous applications in biometrics, security, commercial, military, interaction with computers, and providing services to the individual. In this paper, the age estimation system is divided into four distinct stages. The first step is to extract local features including Gabor wavelets (GW), Local Binary Pattern (LBP), Local Phase Quantization (LPQ), and Histogram of Oriented Gradients (HOG). These attributes are then combined in the second step as a feature fusion method, which combines four different feature extraction methods. In the following step, Particle Swarm Optimization (PSO) as a meta-heuristic optimization algorithm is used to decrease the size of attributes and find optimal features. Finally, we used classification and regression methods to estimate the age and age groups. Initially, we used support vector machines (SVMs) to determine the age class, and then used support vector regression (SVRs) to estimate the ages within those groups. Finally, our algorithm was examined on two widely used databases, i.e. the FG-NET and the MORPH, to determine its effectiveness regarding aging estimates. In the FGNET dataset, we achieved an MAE of 3.34 years and 75.69 percent classification accuracy, and in the MORPH dataset, we obtained an MAE of 3.21 years and 81.66 percent classification accuracy.**

Keywords— Local Binary Pattern Algorithm (LBP), Age Estimation, Gabor Wavelet, Feature Fusion, Local Phase Quantization Algorithm (LPQ), Histogram of Oriented Gradients (HOG), Particle Swarm Optimization (PSO).

I. INTRODUCTION

The human face has many features and characteristics, such as emotions, sex, race, age, etc. According to recent surveys, human faces are crucial to human social interaction, which means faces are essential for daily communication. The technology is widely used for commercial and security purposes. Nowadays, with the increased use of computer and electronic systems, it is thought that these systems may be able to have a human-friendly relationship besides accomplishing their tasks, which is essential for computer systems. It is necessary to recognize the human face and identify its features and characteristics, including emotions and age. In this case, it can effectively communicate with anyone, regardless of age group, and this is one of the most important causes of attention [1]. Some different factors can affect the appearance of the face, such as gravity, exposure to ultraviolet radiation from the sun, reconstruction of bone structure, and facial muscular activity [2]. Another factor that permanently changes the appearance of the face is age. Aging is an unavoidable, unintentional process that manifests itself on the face. Changes in soft tissue and bone structure accompany aging. There are three distinct characteristics of facial aging [3]. First and foremost, aging is inescapable and unavoidable [4]. Aging cannot be prevented or slowed down. Aging is a gradual, irreversible process. Secondly, aging patterns differ from person to person. Genetics and external factors such as health, environmental conditions, and lifestyle influence the aging process. Finally, the obtained models have local time. There is no permanent aging model of the face. In addition, changes over time affect the future appearance of the face and do not influence the past look. Despite the uniqueness of each individual's aging pattern, some common variations and similarities in facial growth can be modeled [5]. From childhood to adolescence, facial changes are primarily related to facial size and shape, while from youth to aging, most changes are related to changes in skin texture and facial color. The facial skin becomes less elastic and wrinkled by the loss of collagen under the skin and also by darker, more elastic forces [6].

Automatic age estimation methods work based on the classifier of input images according to predicted age. The system generally begins to work by receiving a photo of someone's face and then proceeds through the various stages, analyzing its features to determine the approximate age or age category of the person concerned. There are three main types of features: local, global, or hybrid. As the first batch of features, local features are extracted from different facial regions. Local features include wrinkles and the relative position of facial members. The second group, global characteristics, consists of diverse individual features including personality, feelings, ethnicity, sex, and race. These features can be used to accurately estimate age. The third type of feature is hybrid. As the name implies, these characteristics are derived from a combination of local and global features, which include both individual and age characteristics.

This work introduces a novel age estimation system based on a combination of local features such as LBP, LPQ, HOG, and GABOR. The local features have been used to extract features such as skin spots and wrinkles. Then, as an optimization algorithm, PSO is utilized to find optimal features while removing redundant and irrelevant attributes. In addition, we used hierarchical estimation. First, we divided the input data into four age groups using an SVM classifier, and then we used a proper regressor to estimate the numerical age of each instance. We investigated the efficiency of the proposed method on two well-known databases, FG-NET and MORPH album 2. FG-NET has diverse face images, including lighting, blur, and expressions. It includes 1002 images of 82 different people ranging in age from 0 to 69

978-1-6654-0208-8/21/$31.00 ©2021 IEEE

years, with half of them being in the range of 0 and 13 years. The MORPH dataset contains 55,000 unique images of over 13,000 people ages between 16 and 77 years. Each individual has an average of four images. The remainder of this study is structured as follows. Section II describes the related works. Section III discusses the material's specifics and proposed methods. Also, section IV presents the experimental results, while section V summarizes the conclusion and recommendations.

II. REVIEW OF THE RELATED LITERATURE

Previous work in age estimation using facial images can be categorized into two classes: multi-class methods and regression approaches. The first group uses each age as a class label, while the second method estimates the specific age.

There are several methods for estimating age, including classification, regression, and ranking. To complete the age estimation task, various feature extraction methods can be used in combination with age estimation techniques. Many excellent approaches have appeared in recent years. Over the last decade, there have been a lot of successful approaches. One of the oldest researches in this area is the Lobo [7] article. Based on anthropometry and wrinkle patterns, Lobo et al. assigned the images to three categories: babies, young adults, and seniors. Wrinkle patterns were extracted from areas such as the forehead, cheeks, and corners of the eye. The accuracy of children group classification was less than 68 percent. Ramanathan and Chellappa [8] consider a craniofacial growth model and calculate eight distance ratios to model age progression. They used 233 images, of which 109 of them were from the FG-NET dataset, and others were from the private dataset. They reported progress in face recognition from 8% to 15%.

Lanitis [9] represented age as a function Age = f (b). An age function determines the interaction of age with model parameters. In this case, age represents a true estimated age, b has two parameters from AAM. AAM can be applied to any age, and AAM considers both geometry and texture. Fine wrinkles and skin details are not included in the AAM model. They illustrated an improvement in the age group from 63% up to 71%. Han et al. [10] offered a hierarchical age estimation and studied the effect of aging on facial components. They assessed the performance of humans and machines in estimating demographics (age, gender, and ethnicity). They extracted BIF and demographic informative features from facial images. They used BIF and demographic characteristics that are obtained from facial images. The effectiveness of this method is examined using the mean of absolute errors (MAE) and the cumulative score (CS). They achieved 78% CS and 3.8 years MAE in the FG-NET dataset and 77.4% CS and 3.6 years MAE in the MORPH II dataset.

Juha Ylioinas et al. [11] model completed local binary patterns (CLBPs) using a support vector regressor (SVR). This method first adjusts the face alignment according to the shape and position of the face. Similarity conversion is based on local binary pattern distributions. They obtained 5.09 years of mean absolute error (MAE). Gunay et al. [12] described aging using hybrid features, AAM, LBP, and GABOR. Furthermore, they used SVM to build a model for age estimation. They considered a hierarchical approach, so they used SVM to estimate the age group first, then a regression to estimate the real age within the age group. Their method obtained 4.13 years of MAE on the FG-NET dataset. Akinyemi and Onifade [13] proposed the ethnic-specific age group ranking for predicting age. They performed this method on the FG-NET dataset and reported an MAE of 3.18 years. Obtained results demonstrate that ethnicity parameters increase the efficiency of the age prediction system.

III. MATERIAL AND PROPOSED METHODS

A. Dataset

To assess the efficacy of the age estimation algorithm, we need a database with a high statistical population. In this paper, two popular datasets are used: FG-NET and MORPH album 2.

The FGNET dataset includes 1002 facial images of 82 persons between the ages of 0 and 69 years, with an average of 12 images for each person. This database is unbalanced because half of the instances are younger than 13 years old. The photos, which are both color and greyscale, have an average resolution of 384x487 pixels. Also, there is extreme diversity in the pose, facial expression, blur, and lighting. Figure I displays some examples of the FG-NET dataset.

Figure I. Facial image example of FG-NET dataset

The Age Group at the University of Northern California created the MORPH dataset, which is freely available to the public. This dataset is split into two parts. Race, sex, birth date, and age are all included in both categories. The MORPH album 2 includes 55,608 images of 13000 persons ranging in age from 16 to 77. The average dimension of these images is 400x480 pixels. Fig. II displays a few examples from the MORPH album 2 dataset.

Figure II. Facial image example of MORPH dataset

B. Proposed Method

The proposed approach includes six main steps: image preprocessing, feature extraction, normalization, feature fusion, feature selection, and age estimation. This paper presents a system that uses local features to estimate age from facial images. Preprocessing and normalization of input images are required. All of the extracted features are combined to take into account all information. Also, because of the large number of features that consume a significant amount of time and memory during the process, the PSO algorithm is utilized as a feature selection method to select the optimal features while also removing noisy attributes. Moreover, in this study, a hierarchical age estimation approach is proposed. As a result, the images are first categorized into various age groups using a support vector machine (SVM). Finally, using support vector regression (SVR), the exact age within the specific age group is estimated. Figure III summarizes our proposed approach.

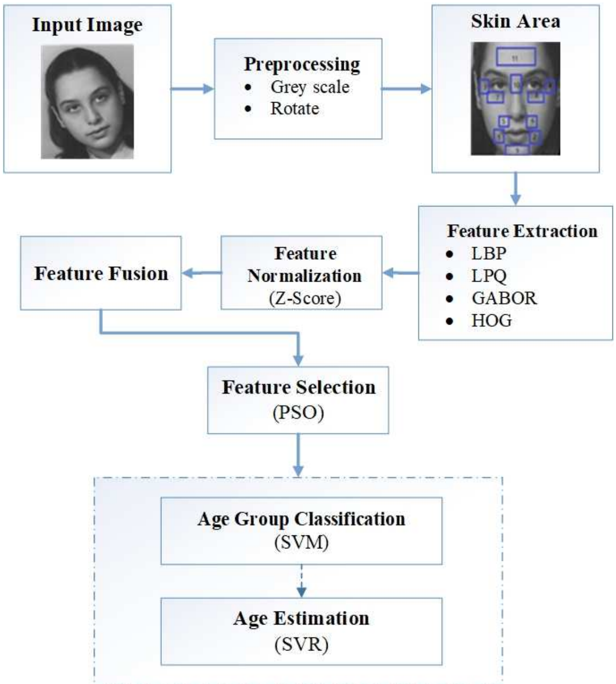

Figure III. Summary of the proposed system for age estimation

C. Preprocessing

It should be mentioned that the datasets include several different images such as diversity in color, blur, expression, pose, and scale. The FG-NET images, for example, were captured using a variety of methods, including image scanning and photographs taken with digital cameras. Some of them are colorful, while others are grayscale. Meanwhile, the images in MORPH Album 2 were gathered from mugshots, so they were not taken under controlled conditions, as they were in FG-NET. As a result, multiple steps must be taken to address this issue. First of all, all the images are converted to grayscale in order to reduce time-consuming and memory usage. Besides, to improve the accuracy of the location of the skin areas to extract local characteristics, every image should be normalized according to the center of two eyes and scaled to the same inter-pupillary distance. The angle of the face is then rotated to the horizontal line using the center of the eyes in the second step. If it deviates from the horizon line, it turns to maintain the pose in a straight line, and then a median filter is employed to remove image noise. Lastly, the Viola-Jones face detector [14] is utilized to locate and crop the face. The image is eventually resized to 240x300 pixels.

D. Skin Area

Local features are significant to describe the wrinkle, spot, and texture of the skin. Wrinkles and spots appear in some areas such as the corner of the eyes and mouth, forehead, nose, and cheeks. Lemperle et al. [15] have described zones that consist of most wrinkles. A number of facial characteristics, including the angle of the eyes and the distance between the mouth and nose, have been recognized as significantly correlated with aging. Meanwhile, focusing on the areas that have experienced the most changes during the aging process will help to eliminate unnecessary areas. According to [15], the following skin areas were chosen for the aging process: the corners of the eyes, chin, mouth, nose, cheekbones, top of the nose, and the forehead. A total of eleven areas are chosen for defining skin areas. An example of selected skin areas of 15 years old instance is shown in Figure IV. After that, it is necessary to crop the skin area when they are defined. It is crucial for normalization because it removes unnecessary parts while preserving local features that are relevant for skin analysis.

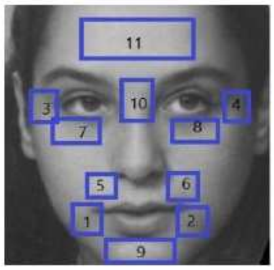

1. Left corner of the mouth lines
2. Right corner of the mouth lines
3. Left periorbital lines
4. Right periorbital lines
5. Left nasolabial folds
6. Right nasolabial folds
7. Left cheek lines
8. Right cheek lines
9. Chin crease
10. Top nose
11. Horizontal forehead lines

Figure IV. A sample of a 15-year-old's cropped skin

E. Local Feature Description

Local features are obtained using the LBP, LPQ, HOG, and Gabor Algorithms.

1) Local Binary Pattern (LBP): The Local Binary Pattern algorithm (LBP) was invented in 1994. The LBP algorithm is widely applied for texture classification, face analysis, motion analysis, facial description, sex, and identifying an age group. Aging skin has very details, so the texture features are extracted using the LBP method. LBP technique can detect microstructure patterns such as spots, lines, edges, and flat areas on the skin [16]. Based on LBP, each pixel is assigned a value that is compared with its neighbors. The LBP code can be defined as follows:

$$LBP_{P,R} = \sum_{p=0}^{p-1} s(g_p - g_c)2^P \tag{1}$$

Where P denotes the number of neighboring pixels, and the distance between the center and the neighboring pixels is represented by R. Also, g_p and g_c show gray-level values of the central pixels and P surrounding pixels, respectively. The function s is expressed by:

$$s(x) = f(x) = \begin{cases} 0 & ,x < 0 \\ 1 & ,x \geq 0 \end{cases} \tag{2}$$

2) Local Phase Quantization (LPQ): The local phase quantization operator (LPQ) was first proposed by Heikkila [17]. The LPQ is utilized as an image descriptor that is based on the blur invariance property in Fourier processing. The LPQ strategy uses local phase data that phase is inspected over a square neighborhood N_x of size M by M:

$$F(u,x) = \sum_{y \in N_x} f(x-y)e^{-j2\pi u^T y} = w_u^T f_x \tag{3}$$

Where w_u is the vector of the 2D DFT at a frequency of u, and f_x is a vector including whole images from N_x. Four frequency points are considered in LPQ : u_1=[a,0]^T, u_2=[0,a]^T, u_3=[a,a]^T, and u_4=[a,-a]^T, where a is the adequately small scalar. An F_x vector is generated for each pixel position:

$$F_x = [F(u_1, x) + \mathrm{F}(u_2, x) + \mathrm{F}(u_3, x) + \mathrm{F}(u_4, x)] \quad (4)$$

Afterward, the phase information is obtained by considering the sign of the real and imaginary part of each Fourier coefficient as a binary coefficient. As a result, these binary values are expressed as integer numbers ranging from 0 to 255.

3) Histogram of Oriented Gradients (HOG): Histogram of Oriented Gradient (HOG) is one of the most significant feature extractors that is used to recognize objects in many different applications [18]. It is employed to extract the magnitude and edge orientation of an image. Therefore, the general method of HOG is to first divide an image into smaller parts called cells, then a histogram of edge orientation is computed for each one. In the first step, the image gradients are computed by using the following filter kernel [19]:

$$g_x = [1,0,-1] \quad (5)$$

$$g_y = [1,0,-1]^T \quad (6)$$

The next stage is to create cell histograms. The cells could have a rectangular or radial shape. Furthermore, histograms are equally distributed between 0 and 180 degrees as well as 0 and 360 degrees, depending on whether the gradient is "unsigned" or "signed." Histogram counts are normalized to offset the illumination, then use the results obtained to normalize every cell within the block. The blocks are normalized as follows:

$$L1-norm\colon u \rightarrow {}^{u}\!/_{(\| u \|_1 + \epsilon)} \quad (7)$$

$$L1-sqrt\colon u \rightarrow \sqrt{{}^{u}\!/_{(\| u \|_1 + \epsilon)}} \quad (8)$$

$$L2-norm\colon u \rightarrow {}^{u}\!\Big/_{\sqrt{{}^{u}/_{(\| u \|_2^2 + \epsilon^2)}}} \quad (9)$$

$L2-hys\colon L2-norm, plus\ clipping\ at\ .2$ and renormalizing (10)

Where u is the non-normalized vector containing all histograms in a given block, ||v||k is k-norm for k=1, 2 and ∈ is a small constant. Finally, the integration of these histograms illustrates the HOG model.

4) Gabor Wavelet: For estimating age, a facial wrinkle is one of the most valuable features. Wrinkles form for a variety of reasons and can develop in a variety of directions. For example, it may create wrinkle lines based on muscle movements or facial expressions in a smiling mood. The essential point is that each wrinkle is unique. As a result, it could be used in an age estimation system. Therefore, the Gabor filter is used to extract wrinkle and texture characteristics. A further benefit of Gabor wavelets is their ability to extract specific information about the facial area [20]. Gabor filters produce features with considerably large dimensional space, making all subsequent computations costly. Solving this issue can be achieved by reducing dimensionality with the PSO algorithm. A sample of the Gabor filter is shown in Figure V.

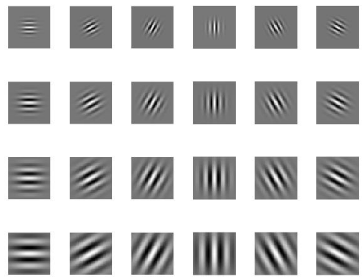

Figure V. Gabor filter with 4 scales and 6 orientations.

F. Normalization

In this paper, we use the z- score to normalize the extracted features [21]. Z-scores are applied in the statistics for comparing the means of homogeneous datasets. Analyzing data is much easier when they are normalized. In order to normalize data using Z-score, first the mean and standard deviation are computed, then the normalized data is determined by the following equation:

$$f'_i = \frac{f_i - \mu_i}{\sigma_i}, \ \ i = LBP, LPQ, HOG, \ldots \quad (17)$$

Where f_i is the i_{th} feature vector, μ_i and σ_i represent the mean and the standard deviation of the i_{th} feature, respectively. The normalized feature vector is shown by f'_i.

G. Feature Fusion

The integration and combination of features [22] have been used effectively in several fields such as biometric security, facial recognition, photos, etc. Due to that, each feature vector contains specific information, combining characteristics can create a comprehensive set of features. Therefore, a feature fusion method is employed to combine the extracted features and provide an informative set of normalized local features.

$$f_{fused} = \left(f'_{LBP} f'_{LPQ} f'_{HOG} f'_{Gabor}\right) = (c_1, \ldots, c_k, w_1, \ldots, w_l, t1_1, \ldots, t1_m, t2_1, \ldots, t2_n) \quad (18)$$

Where f_{fused} refers to the combined feature vector that will be utilized in the reduction of dimensionality stage, as discussed in the following section.

H. Feature Selection

Particle Swarm Optimization (PSO) is a swarm intelligence algorithm proposed by Kennedy and Eberhart [23]. PSO is well-known for fast exploration and exploitation in the search space. The PSO algorithm starts with an initial random population of a candidate solution. Each element of the population is called a particle. The PSO algorithm consists of a finite number of particles randomly initialized, and each particle has the potential of being a proper solution.

These particles move in the search space according to formulation over the particle's position. The local value of each particle influences its movement, and its purpose is to achieve the best position in the search domain by utilizing the superior position discovered by other particles. Each iteration determines the best value by evaluating position and velocity vectors [24]. The best value is saved in the Pbest matrix, and its position is stored as the global best (Gbest). The iteration is repeated, and the last updated best position is considered as an optimum value. Particle position and velocity are updated as follows:

$$V_{i,j}(t+1) = V_{i,j}(t) + c_1 r_1 * \left[P_{best_{i,j}}(t) - X_{i,j}(t)\right] + c_2 r_2 * [g_{best}(t) - X_{i,j}(t)] \quad (19)$$

$$X_{i,j}(t+1) = X_{i,j}(t) + V_{i,j}(t+1), \quad i = 1,2,\dots,M; \; J = 1,2,\dots,N \quad (20)$$

Where c_1 and c_2 parameters are selected between [0-2]. Also, r_1 and r_2 are random coefficient and normal distributed between [0-1]. P_{best} and G_{best} matrices are represented according to the following:

N: *number of search space*
M: *number of particle*
$i =$ *particle index*
$j =$ *dimension number*
$X =$ *position matrix*
$V =$ *velocity matrix*

$$X_{i,j} = \begin{bmatrix} X_{11} & X_{12} & \cdots & X_{1N} \\ \vdots & & \ddots & \vdots \\ X_{M1} & X_{M2} & \cdots & X_{MN} \end{bmatrix} \quad (21)$$

$$V_{i,j} = \begin{bmatrix} V_{11} & V_{12} & \cdots & V_{1N} \\ \vdots & & \ddots & \vdots \\ V_{M1} & V_{M2} & \cdots & V_{MN} \end{bmatrix} \quad (22)$$

$$P_{best_{i,j}} \begin{bmatrix} P_{best_{11}} & P_{best_{12}} & \cdots & P_{best_{1N}} \\ \vdots & & \ddots & \vdots \\ P_{best_{M1}} & P_{best_{M2}} & \cdots & P_{best_{MN}} \end{bmatrix} \quad (23)$$

$$G_{best} = [G_{best_1} \; G_{best_2} \; \dots \; G_{best_N}] \quad (24)$$

I. Age Estimation

Depending on the age group, the aging process may be different. For instance, wrinkles commonly exist in adulthood, whereas geometric features alter during growing up. To decrease the errors associated with single-level age estimation, a hierarchical approach has been proposed in the existing literature. A hierarchical method is Combining an age group classifier and an age estimator. The proposed work first uses an SVM to categorize a facial image into a determined age category and then uses an SVR to define an accurate age estimation.

IV. Experimental Results and Discussion

In this study, all experiments were repeated 50 times independently, which allowed for more accurate results. Moreover, all algorithms are implemented using MATLAB R2018b with an Intel Core i7 processor, 2.2 GHz CPU, and 12 GB of RAM.

A. Evaluation Metrics

The performance of the proposed method is assessed using the MAE. The MAE between the predicted age (a') and the actual age (a) are calculated. Where N is the total number of test images.

$$MAE = \sum_{i=1}^{N} \frac{|a' - a|}{N} \quad (25)$$

B. Evaluation Protocols

A uniform split of 80% was used for training and 20% was used for testing to conduct both FG-NET and MORPH experiments. By using 10-fold cross-validation with using RBF kernel, the parameters of the SVM and SVR are determined. Both classification and regression were done using the LIBSVM library [25].

C. Experimental Results

We demonstrate the effectiveness of the proposed age estimation system based on the MAE using the FG-NET dataset and the MORPH album 2 dataset in this section.

1) Results on FG-NET Database:

Based on the distribution of data, four age categories have been defined in order to ensure a sufficient number of training data as well as testing data. It leads to having various groups for kids, adolescents, adults, and elders, which is particularly beneficial to have a wide range of ages. Table I shows the defined classes and data distribution.

The system's performance was evaluated using various combinations of local features. Table II presents the performance in terms of the MAE and accuracy of classification. The lowest MAE of 3.34 and the highest accuracy of 75.69% were obtained for a combination of local features (LBP+LPQ+ HOG+GABOR).

TABLE I. The Number of Training and Testing Data of FG-NET Dataset

Class	Age Range	Number of Training Data	Number of Testing Data
A	0-13	149	42
B	14-21	169	45
C	22-39	147	20
D	40-69	43	20

2) Results on MORPH album 2 database:

Samples are divided into four age groups for age group classification: kids, adolescents, adults, and elders. The defined groups and data distribution for the MORPH dataset (album 2) are displayed in Table III. To obtain the best performance, we used the Feature Fusion method which combined the local features. Table IV shows the performance in terms of MAE and accuracy of classification. This is clear that the lowest MAE of 3.21 and the highest accuracy of

81.66% were achieved for the combination of local features (LBP+LPQ+HOG+ GABOR).

TABLE II. RESULTS OF THE PROPOSED METHOD IN VARIOUS FEATURE SETS ON THE FG-NET DATASET

Features	MAE (years)	Classification Accuracy (%)
GABOR	4.05	21.25%
LPQ	3.81	22.83%
LBP	3.97	44.87%
HOG	3.41	35.01%
GABOR+LBP	3.79	58.06%
GABOR+LPQ	3.83	59.67%
GABOR+HOG	3.69	33.25%
LBP+LPQ	3.39	65.32%
LBP+HOG	3.79	44.35%
LPQ+HOG	3.88	47.58%
LBP+HOG+GABOR	3.68	56.45%
LPQ+HOG+GABOR	3.67	51.64%
LBP+LPQ+HOG+GABOR	**3.34**	**75.69%**

TABLE III. THE NUMBER OF TRAINING AND TESTING DATA OF MORPH DATASET

Class	Age Range	Number of Training Data	Number of Testing Data
A	16-25	193	39
B	26-35	188	44
C	36-45	166	62
D	Up 46	183	38

D. Comparison to other approaches

In this part, we compare the proposed method with different methods including RED-SVM [26], DEX [27], Group-Aware [28], and GPR [29] on FG-NET and MORPH album 2 databases. The results of all comparative methods have been shown regarding MAE on FG-NET and MORPH datasets in Table V. Our proposed framework demonstrated superior performance than all other approaches on both datasets, FG-NET and MORPH because it used not only combined features but also optimal features without redundancies. As the results show, our approach outperforms several approaches in terms of MAE. It should be mentioned that the use of PSO for feature selection as well as hierarchical classification leads to achieving better results.

TABLE IV. RESULTS OF THE PROPOSED METHOD IN VARIOUS FEATURE SETS ON THE MORPH DATASET

Features	MAE (years)	Classification Accuracy (%)
GABOR	3.96	18.33%
LPQ	3.75	54.44%
LBP	3.71	72.22%
HOG	3.94	25.68%
GABOR+LBP	3.93	66.11%
GABOR+LPQ	3.64	55.55%
GABOR+HOG	3.71	69.94%
LBP+LPQ	3.97	36.66%
LBP+HOG	3.91	67.77%
LPQ+HOG	3.73	53.33%
LBP+HOG+GABOR	3.77	62.22%
LPQ+HOG+GABOR	3.81	76.37%
LBP+LPQ+HOG+GABOR	**3.21**	**81.66%**

TABLE V. COMPARISON BETWEEN THE PROPOSED ALGORITHM AND OTHER APPROACHES IN TERMS OF MAE(YEARS)

Features	FG-NET	MORPH
RED-SVM	5.24	6.49
GPR	4.41	3.7
DEX	4.63	3.25
GROUP-Aware	3.93	3.25
Proposed Method	**3.34**	**3.21**

V. CONCLUSION

We proposed a new framework for age estimation using local features and a hierarchical classifier. In this research study, we used PSO as a meta-heuristic algorithm for feature selection. Furthermore, a variety of feature combinations of local features with different settings have also been investigated. The performance of the system is enhanced by using a large number of feature extractors. Skin features are extracted using LBP. Also, GABOR and HOG are useful for extracting wrinkle features. The LPQ features have demonstrated that they are incredibly resistant to lightning and blur. Meanwhile, PSO eliminates redundant and irrelevant features by selecting the most informative features. The proposed method performed better than the previous methods, as shown by the experimental results. Although the proposed method has good performance, some factors such as lack of data in some ages and various conditions such as light and expression can affect the efficiency of the proposed approach.

VI. References

[1] W. Pei, H. Dibeklioğlu, T. Baltrušaitis, and D. M. Tax, "Attended end-to-end architecture for age estimation from facial expression videos," *IEEE Transactions on Image Processing,* vol. 29, pp. 1972-1984, 2019.

[2] R. Angulu, J. R. Tapamo, and A. O. Adewumi, "Age estimation via face images: a survey," *EURASIP Journal on Image and Video Processing,* vol. 2018, no. 1, pp. 1-35, 2018.

[3] X. Geng, Q. Wang, and Y. Xia, "Facial age estimation by adaptive label distribution learning," in *2014 22nd International Conference on Pattern Recognition*, IEEE, pp. 4465-4470, 2014.

[4] R. Angulu, J. R. Tapamo, and A. O. Adewumi, "Age-group estimation using feature and decision level fusion," *The Computer Journal,* vol. 62, no. 3, pp. 346-358, 2019.

[5] A. S. Al-Shannaq and L. A. Elrefaei, "Comprehensive analysis of the literature for age estimation from facial images," *IEEE Access,* vol. 7, pp. 93229-93249, 2019.

[6] J. K. Pontes, A. S. Britto Jr, C. Fookes, and A. L. Koerich, "A flexible hierarchical approach for facial age estimation based on multiple features," *Pattern Recognition,* vol. 54, pp. 34-51, 2016.

[7] Y. H. Kwon and N. da Vitoria Lobo, "Age classification from facial images," *Computer vision and image understanding,* vol. 74, no. 1, pp. 1-21, 1999.

[8] N. Ramanathan and R. Chellappa, "Modeling age progression in young faces," in *2006 IEEE Computer Society Conference on Computer Vision and Pattern Recognition (CVPR'06)*, vol. 1: IEEE, pp. 387-394, 2006.

[9] A. Lanitis, C. J. Taylor, and T. F. Cootes, "Toward automatic simulation of aging effects on face images," *IEEE Transactions on pattern Analysis and machine Intelligence,* vol. 24, no. 4, pp. 442-455, 2002.

[10] H. Han, C. Otto, X. Liu, and A. K. Jain, "Demographic estimation from face images: Human vs. machine performance," *IEEE transactions on pattern analysis and machine intelligence,* vol. 37, no. 6, pp. 1148-1161, 2014.

[11] J. Ylioinas, A. Hadid, X. Hong, and M. Pietikäinen, "Age estimation using local binary pattern kernel density estimate," in *International Conference on Image Analysis and Processing*, Springer, pp. 141-150, 2013.

[12] A. Gunay and V. V. Nabiyev, "Facial age estimation based on decision level fusion of amm, lbp and gabor features," *Int. J. Adv. Comput. Sci. Appl,* vol. 6, pp. 19-26, 2015.

[13] J. D. Akinyemi and O. F. Onifade, "An ethnic-specific age group ranking approach to facial age estimation using raw pixel features," in *2016 IEEE Symposium on Technologies for Homeland Security (HST)*, IEEE, pp. 1-6, 2016.

[14] P. Viola and M. Jones, "Robust real-time object detection," *International journal of computer vision,* vol. 4, no. 34-47, p. 4, 2001.

[15] G. Lemperle, "A classification of facial wrinkles," 2015.

[16] T. Ojala, M. Pietikäinen, and D. Harwood, "A comparative study of texture measures with classification based on featured distributions," *Pattern recognition,* vol. 29, no. 1, pp. 51-59, 1996.

[17] T. Ahonen, E. Rahtu, V. Ojansivu, and J. Heikkila, "Recognition of blurred faces using local phase quantization," in *2008 19th international conference on pattern recognition*, IEEE, pp. 1-4, 2008.

[18] W. R. Schwartz, A. Kembhavi, D. Harwood, and L. S. Davis, "Human detection using partial least squares analysis," in *2009 IEEE 12th international conference on computer vision*, IEEE, pp. 24-31, 2009.

[19] I. Huerta, C. Fernández, and A. Prati, "Facial age estimation through the fusion of texture and local appearance descriptors," in *European conference on computer vision*, Springer, pp. 667-681. 2014.

[20] M. Bereta, P. Karczmarek, W. Pedrycz, and M. Reformat, "Local descriptors in application to the aging problem in face recognition," *Pattern Recognition,* vol. 46, no. 10, pp. 2634-2646, 2013.

[21] A. Ross and R. Govindarajan, "Feature level fusion in biometric systems," in *proceedings of Biometric Consortium Conference (BCC)*, pp. 1-2, 2014.

[22] J. Yang, J.-y. Yang, D. Zhang, and J.-f. Lu, "Feature fusion: parallel strategy vs. serial strategy," *Pattern recognition,* vol. 36, no. 6, pp. 1369-1381, 2003.

[23] J. Kennedy and R. Eberhart, "Particle swarm optimization," in *Proceedings of ICNN'95-international conference on neural networks*, vol. 4: IEEE, pp. 1942-1948, 1995.

[24] M. Sharif, J. Amin, M. Raza, M. Yasmin, and S. C. Satapathy, "An integrated design of particle swarm optimization (PSO) with fusion of features for detection of brain tumor," *Pattern Recognition Letters,* vol. 129, pp. 150-157, 2020.

[25] C.-C. Chang and C.-J. Lin, "LIBSVM: a library for support vector machines," *ACM transactions on intelligent systems and technology (TIST),* vol. 2, no. 3, pp. 1-27, 2011.

[26] K.-Y. Chang, C.-S. Chen, and Y.-P. Hung, "A ranking approach for human ages estimation based on face images," in *2010 20th International Conference on Pattern Recognition*, IEEE, pp. 3396-3399, 2010.

[27] R. Rothe, R. Timofte, and L. Van Gool, "Deep expectation of real and apparent age from a single image without facial landmarks," *International Journal of Computer Vision,* vol. 126, no. 2, pp. 144-157, 2018.

[28] Y. Dong, Y. Liu, and S. Lian, "Automatic age estimation based on deep learning algorithm," *Neurocomputing,* vol. 187, pp. 4-10, 2016.

[29] M. M. Sawant and K. Bhurchandi, "Hierarchical facial age estimation using Gaussian process regression," *IEEE Access,* vol. 7, pp. 9142-9152, 2019.